frontiers | Frontiers in Materials

ORIGINAL RESEARCH
published: 05 May 2022
doi: 10.3389/fmats.2022.881229

A Tunable Multifunctional Terahertz Asymmetric Transmission Device Hybrid With Vanadium Dioxide Blocks

Boli Xu , Renbin Zhong , Zekun Liang , Zheng Fang , Jianhui Fang , Huimin Zhang , Zhenhua Wu , Kaichun Zhang , Min Hu and Diwei Liu*

Terahertz Research Center, School of Electronic Science and Engineering, Cooperative Innovation Centre of Terahertz Science, University of Electronic Science and Technology of China, Chengdu, China

A tunable multifunctional terahertz metamaterial asymmetric transmission device is proposed. The device is composed of three layers from top to bottom, i.e., Ge–SiO_2–Ge. The germanium layer with a VO_2 block enables it to work in two operating modes by controlling the state of the VO_2 blocks, thereby flexibly realizing asymmetric forward and backward transmission with specific polarization. The device is endowed with a more flexible design of electromagnetic systems, rendering it suitable for applications in polarization converters, polarization filters, and other polarization modulators.

Keywords: terahertz, meta-materials, multifunctional, asymmetric transmission, vanadium dioxide

OPEN ACCESS

Edited by:
Jinfeng Zhu,
Xiamen University, China

Reviewed by:
Jianqiang Gu,
Tianjin University, China
Zhanghua Han,
Shandong Normal University, China

****Correspondence:***
Renbin Zhong
rbzhong@uestc.edu.cn

Specialty section:
This article was submitted to Metamaterials, a section of the journal Frontiers in Materials

Received: *22 February 2022*
Accepted: *06 April 2022*
Published: *05 May 2022*

Citation:
Xu B, Zhong R, Liang Z, Fang Z, Fang J, Zhang H, Wu Z, Zhang K, Hu M and Liu D (2022) A Tunable Multifunctional Terahertz Asymmetric Transmission Device Hybrid With Vanadium Dioxide Blocks. Front. Mater. 9:881229. doi: 10.3389/fmats.2022.881229

INTRODUCTION

Terahertz (THz) waves with frequencies between 0.1 and 10 THz have been widely recognized for their high-speed and large-capacity wireless communication capability (Shao, 2015; Suen, 2016), among which tunable asymmetric transmission devices demonstrate application significance. In 2006, Fedotov et al. realized the asymmetric transmission of chiral materials for the first time (Fedotov, 2006). Asymmetric transmission devices are widely used as photodiodes, circulators and isolators in fields such as chiral spectroscopy, ultrafast information processing, optical interconnection, and communication (Zhang, 2017; Zheng, 2009).

Tunable asymmetric transmission devices are desired in complex and changeable information communication. Existing modulation asymmetric transmission devices include a planar chiral metamaterial based on graphene developed by Huang (2017) dynamic metamaterial based on a Dirac semi-metal developed by Dai (2019) and a THz Fano resonator based on liquid crystal developed by Shen (2019). These researchers have realized the regulation of asymmetric transmission devices; however, their regulation ideas are aimed at the regulation of asymmetric transmission with or without conversion. Existing application scenarios require flexible selection of the electromagnetic wave passing direction.

A flexibly tunable asymmetric transmission device based on VO_2 is proposed herein. The device can not only switch between two asymmetric transmission modes, but also realize the polarization selection of electromagnetic waves in a certain propagation direction, thereby enabling a flexible design for multifunctional and low-complexity electromagnetic control components.

DESIGN AND THEORETICAL ANALYSIS

Figure 1 shows a unit cell of the proposed THz asymmetric transmission metamaterial device, which consists of a three-layers structure of Ge-SiO_2-Ge from top to bottom. The upper

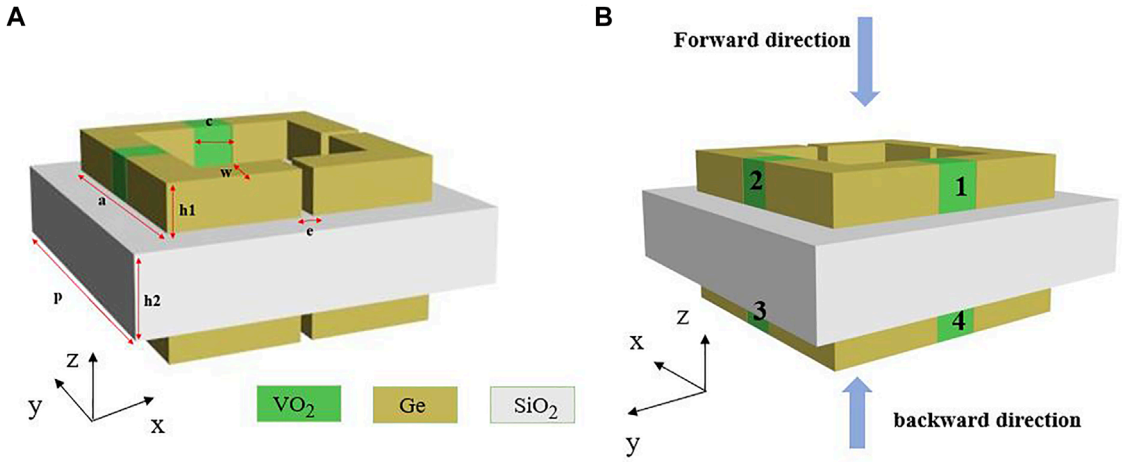

FIGURE 1 | Schematic of the unit cell of the device with P = 120μm, a = 90μm, h1 = c = 25μm, h2 = 15μm, e = 1.155μm, and w = 30μm.

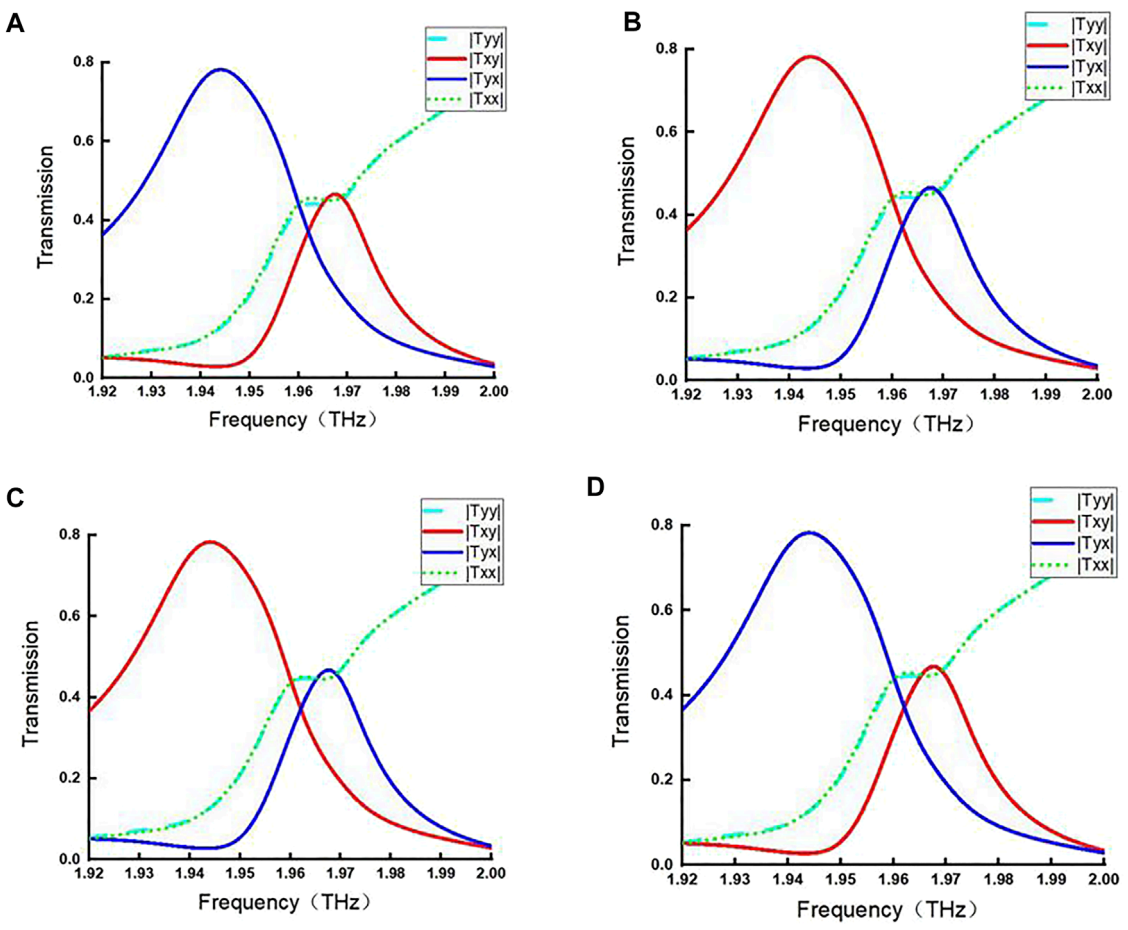

FIGURE 2 | (A) Forward transmission curve on mode I. **(B)** Backward transmission curve on mode I. **(C)** Forward transmission curve on mode II. **(D)** Backward transmission curve on mode II.

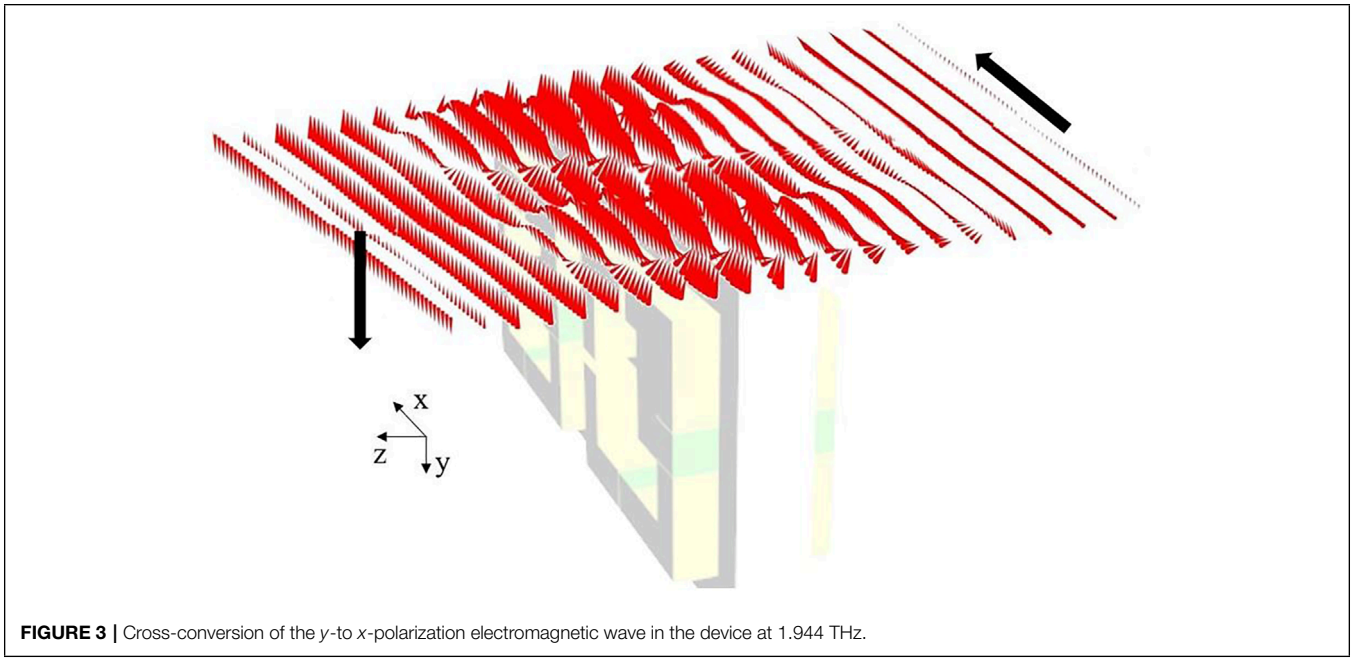

FIGURE 3 | Cross-conversion of the *y*-to *x*-polarization electromagnetic wave in the device at 1.944 THz.

and lower Gelayer are square rings that open at the midpoint of their four sides. For the two rings at the same location, two adjacent openings were filled with VO_2 blocks. The thicknesses of the Ge and SiO_2 layers were $h1 = 25\mu m$ and $h2 = 15\mu m$, respectively. The length of the side of the square ring was $a = 90\mu m$ and the width was $w = 30\mu m$. The geometrical parameters of the unit cell are shown in **Figure 1**.

The relative permittivities of Ge and SiO_2 are 18 and 1.9, respectively (Qin, 2021) The Drude model can be used to effectively characterize the relative permittivity of VO_2 in the THz frequency band, as follows (Li, 2019; Zhu, 2012):

$$\epsilon_{(VO_2)}(\omega) = \epsilon_\infty - \frac{\omega_p^2}{\omega^2 - i\omega\gamma} \tag{1}$$

In **Eq. 1**, the value of ϵ_∞ is 12 and $\gamma = 5.75 \times 10^{13} s^{-1}$. VO_2 exhibits different electromagnetic characteristics in different temperature ranges. It is typically in the insulating and metallic states at temperatures below and above 340 K, respectively (Zhou, 2021). The conductivity of VO_2 in the insulating state is 200 Sm^{-1}, and ω_p is $3.6149 \times 10^{13} rads^{-1}$. When VO_2 is in the metal state, its conductivity is $2 \times 10^5 Sm^{-1}$, and ω_p is $1.143 \times 10^{15} rads^{-1}$.

As shown in **Figure 1B**, we define the forward and backward transmission directions to be along the negative and positive z-axes, respectively. The four blocks of VO_2 are numbered 1 to 4 sequentially from top to bottom. The two operating modes of the device are defined base on the state of the VO_2 blocks: Mode I (M = I), where VO_2 blocks numbered 1 and 3 are in the insulating state, and VO_2 blocks numbered 2 and 4 are in the metal state; Mode II (M = II), where VO_2

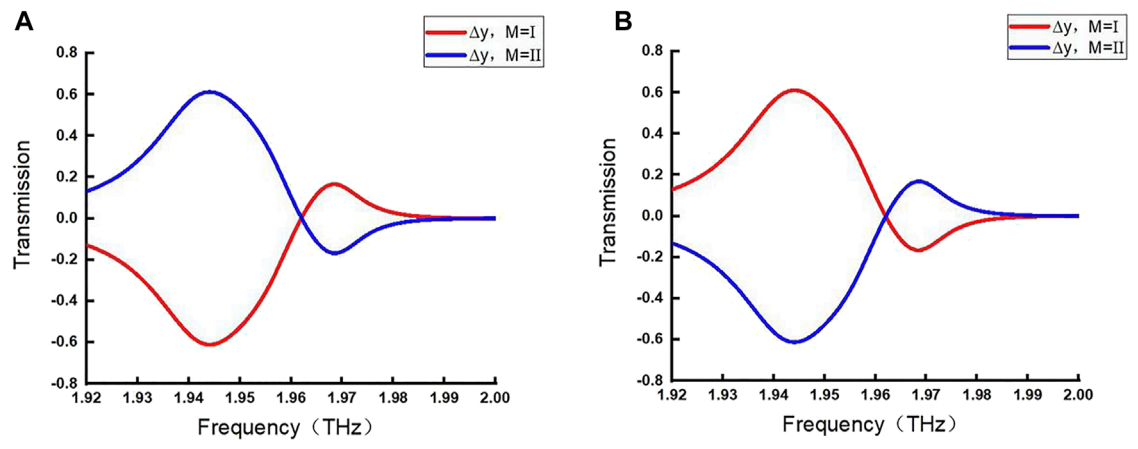

FIGURE 4 | (A) Forward and **(B)** backward asymmetric transmission parameters.

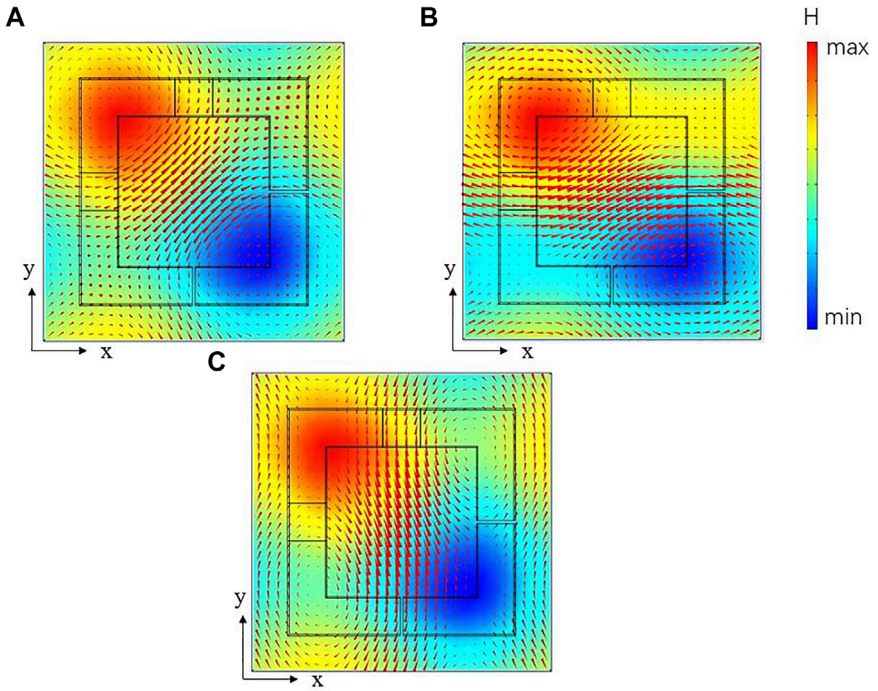

FIGURE 5 | Distribution of magnetic field and surface current at the transmission peak frequencies of **(A)** 1.944 THz, and **(B)** 1.97 THz. **(C)** Distribution of magnetic field, and electric field at 1.944 THz.

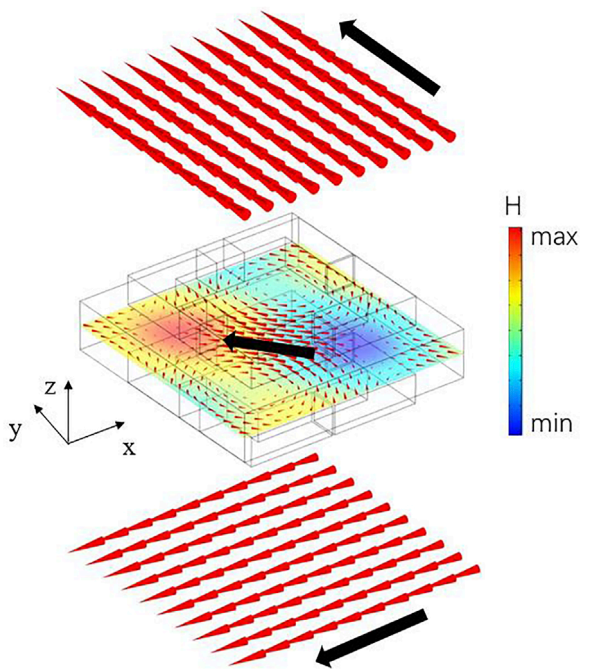

FIGURE 6 | Schematic diagram of cross polarization process between incident and outgoing electromagnetic wave brought by slanting electric field in the device.

blocks numbered 1 and 3 blocks are in the metal state, and VO_2 blocks numbered 2 and 4 are in the insulating state.

The characteristics of the asymmetric transmission of linearly polarized waves are expressed based on the Jones matrix, as follows, Menzel (2010b, 2010a):

$$\begin{pmatrix} T_x \\ -T_y \end{pmatrix} = \begin{pmatrix} T_{xx} & -T_{xy} \\ T_{yx} & T_{yy} \end{pmatrix} \begin{pmatrix} I_x \\ -I_y \end{pmatrix} = T^f \begin{pmatrix} I_x \\ -I_y \end{pmatrix} \tag{2}$$

where I_i and T_i represent the amplitudes of the input and output polarized electromagnetic waves in the i direction, respectively, and T_{ij} denotes the ratio of the amplitude of the input polarized electromagnetic wave in the j direction to that of the output electromagnetic wave in the i direction.

The asymmetric transmission parameters Δ_y and Δ_x can reflect the ability of an asymmetric transmission device. They are defined as the difference in the output electromagnetic wave power between the forward and backward directions, and the wave power can be calculated based on the intensity of polarization transformation (Wang, 2020). In the case of linear polarization, they are expressed as follows:

$$\Delta_y = \left(T_{xy}^f\right)^2 - \left(T_{xy}^b\right)^2 \tag{3}$$

$$\Delta_x = \left(T_{yx}^f\right)^2 - \left(T_{yx}^b\right)^2 \tag{4}$$

The superscripts f and b of T represent forward and backward transmissions, respectively. It is well acknowledged that the

asymmetric transmission of linearly polarized electromagnetic waves is due to the difference between $|T_{xy}|$ and $|T_{yx}|$, where a greater difference between them results in a more significant asymmetric transmission.

RESULTS AND DISCUSSION

Considering a linearly polarized electromagnetic wave, **Figures 2A,B** show the four transmission parameters $|T_{ij}|$ in the forward (−z) and backward (+z) directions, respectively. Generally, in Mode I (M = I), the co-polarization transmission coefficients $|T_{xx}|$ and $|T_{yy}|$ coincide with each other at all frequencies along the forward and backward transmission directions. However, the cross-polarized propagation coefficients $|T_{xy}|$ and $|T_{yx}|$ show a typical reciprocity of the asymmetric transmission device. For instance, in **Figure 2A**, the maximum transmission peak of $|T_{yx}|$ was 0.8 at 1.944 THz, whereas $|T_{xy}|$ was less than 0.03 at the same frequency. The significant difference between $|T_{yx}|$ and $|T_{xy}|$ in the frequency range of 1.92–1.96 THz indicates the excellent asymmetrical transmission characteristic, which is fundamental for the unidirectional transmission of the device.

The device can switch to Mode II (M = II) flexibly by controlling the temperature of VO2 blocks. **Figures 2C,D** show the transmission curves for Mode II. It can be observed that $|T_{xy}|$ is dominant in **Figure 2C**. Furthermore, the trend of curve $|T_{xy}|$ in **Figure 2C** is exactly the same as that of $|T_{yx}|$ in **Figure 2A** for Mode I when forward transmission is considered. The same is observed for $|T_{yx}|$ in **Figure 2D** when compared with $|T_{xy}|$ in **Figure 2B** for backward transmission. However, the co-polarization transmission coefficients $|T_{xx}|$ and $|T_{yy}|$ coincide in the forward and backward transmission directions, regardless of the operating mode. In other words, by controlling the temperature of VO_2, the operating state of the device can be modulated from Mode I to Mode II, thereby allowing asymmetric forward and backward transmissions with specific polarization to be realized flexibly.

Figure 3 shows the forward propagation distribution of the electric field through the device at 1.944 THz. The arrow in the figure indicates the direction of the electric field. As shown, most of the *y*-polarized incident electric fields are rotated 90° to achieve a *x*-polarized output from the device. The cross-conversion between the *y*-and *x*-polarized waves results in high forward transmittance of the *y*-polarized wave in the device.

The asymmetric transmission parameter curves are shown in **Figure 4**. When Δ_y is exceeded zero, forward transmission was greater than backward transmission for the *y*-polarized electromagnetic wave. When the *y*-polarization transmission in the backward direction exceeded that in the forward direction, the value of Δ_y was negative. A larger value of Δ_y indicates a better asymmetric transmission of the device. As shown in **Figure 4A** at Mode II, Δ_y is exceeded zero by a significant extent, and the device allowed a forward transmission of the electromagnetic wave, but not a backward transmission. In Mode I, Δ_y was negative, which indicates that the backward transmission was superior to the forward transmission, and the device allowed a backward transmission but not a forward transmission. The same results can be achieved, as shown in **Figure 4B**, by the same device when

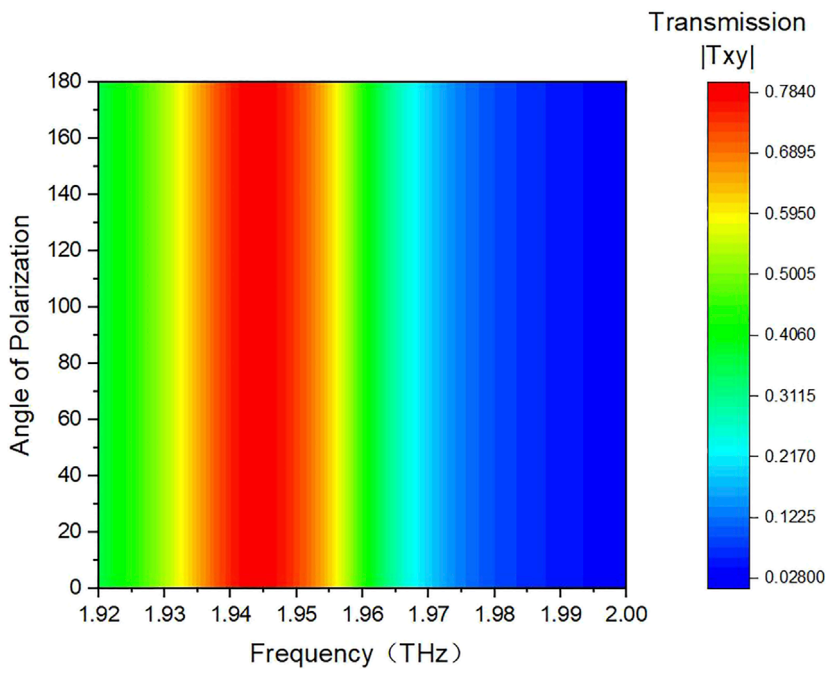

FIGURE 7 | Transmission of the device at different polarization incidence angles.

the incident y-polarized electromagnetic wave propagates along the backward direction.

In general, the device can be used as a *y*- and *x*-polarization converter provided that the operating state is switched from Mode I to Mode II. Furthermore, it can also be used as a polarization selector, a polarization judge, a polarization filter, or another polarization modulator. Hence, methods to miniaturize and fulfill the multifunction requirements of THz application systems can be further devised.

Because the two modes of the device only exchange the forward transmission effect and the reverse transmission effect, the situation when the device works in mode II is analyzed in detail in the following part.

To understand the remarkable asymmetric transmission of the device, **Figure 5** shows the distribution of the electromagnetic field at the center of the device in the xy-plane. In the figures, the color represents the magnetic field amplitude, and the arrow describes the current vector/electric field vector. The distribution of magnetic field and surface current at frequencies of 1.944 THz and 1.97 THz are shown in **Figures 5A,B**, respectively, which corresponding to the transmission peaks frequencies of $|T_{xy}|$ and $|T_{yx}|$. Similar toroidal dipolar resonance can be found, which bring with the high cross-polarization transmission.

Figure 5C is the distribution of magnetic field and electric field (indicated by the arrow) at 1.944 THz. It shows that the electric field vector is centered from the negative magnetic field position to the positive magnetic field position, forming a slanting electric field. Furtherly, the cross-polarization process in the whole space is shown in **Figure 6**. It can be seen that electromagnetic waves incident along *y*-polarization, excite inclined electric field in the device, and finally output *x*-polarized electromagnetic waves. Obviously, the slanting electric field in the device connects the transmission path of the cross-polarized between the incoming and output polarized electromagnetic waves, resulting in a large cross-polarized transmission coefficient $|T_{xy}|$. In order to study the response of the device at different polarization incidence transmission of $|T_{xy}|$.

It can be found in **Figure 7**, that the value of $|T_{xy}|$ is almost insensitive to the polarization angles. According to the above analysis, the same is for the backward transmission of $|T_{xy}|$. So, a stable one-way asymmetric transmission can be realized in the THz frequency band.

CONCLUSION

In conclusion, a flexibly tunable asymmetric transmission device was realized by the position setting and temperature control of VO_2 blocks. The simulation results showed that the device can switch effectively between two operating modes, as well as realize transmission modulation from forward to backward and *y*-polarization to *x*-polarization to control the electromagnetic waves flexibly. The device can be used as a polarization converter, a polarization selector, or another polarization modulator. Furthermore, it can be used to develop flexible designs for photodiodes, polarization detection devices, and other electromagnetic functional devices.

DATA AVAILABILITY STATEMENT

The original contributions presented in the study are included in the article/Supplementary Material, further inquiries can be directed to the corresponding author.

AUTHOR CONTRIBUTIONS

All authors listed have made a substantial, direct, and intellectual contribution to the work and approved it for publication.

FUNDING

This paper was supported by the National Key Research and Development Program of China (No. 2018YFF01013001 and 2017YFA0701000) and the National Natural Science Foundation of China (No. 61988102, 61921002, and 62071108).

REFERENCES

Dai, L., Zhang, Y., O'Hara, J. F., and Zhang, H. (2019). Controllable Broadband Asymmetric Transmission of Terahertz Wave Based on Dirac Semimetals. *Opt. Express* 27, 35784–35796. doi:10.1364/oe.27.035784

Fedotov, V. A. (2006). Circular Conversion Dichroism in Planar Chiral Metamaterials. *Arxiv Org.*

Huang, Y., Yao, Z., Hu, F., Liu, C., Yu, L., Jin, Y., et al. (2017). Tunable Circular Polarization Conversion and Asymmetric Transmission of Planar Chiral Graphene-Metamaterial in Terahertz Region. *Carbon* 119, 305–313. doi:10.1016/j.carbon.2017.04.037

Li, X. (2019). Switchable Multifunctional Terahertz Metasurfaces Employing Vanadium Dioxide. *Scientific Rep.* 9, 5454. doi:10.1038/s41598-019-41915-6

Menzel, C., Helgert, C., Rockstuhl, C., Kley, E. B., Tünnermann, A., Pertsch, T., et al. (2010b). Asymmetric Transmission of Linearly Polarized Light at Optical Metamaterials. *Phys. Rev. Lett.* 104, 253902. doi:10.1103/PhysRevLett.104.253902

Menzel, C. (2010a). Advanced jones Calculus for the Classification of Periodic Metamaterials. *Phys. Rev. A* 82, 053811. doi:10.1103/physreva.82.053811

Qin, C. H. (2021). Enhanced Asymmetric Transmission of Linearly Polarized Light Based on All-Dielectric Stereometamaterial. *J. Opt.* 23. doi:10.1088/2040-8986/abd9df

Shao, T., Shams, H., Anandarajah, P. M., Fice, M. J., Renaud, C. C., van Dijk, F., et al. (2015). Phase Noise Investigation of Multicarrier Sub-thz Wireless Transmission System Based on an Injection-Locked Gain-Switched Laser. *IEEE Trans. Thz Sci. Technol.* 5, 590–597. doi:10.1109/tthz.2015.2418996

Shen, Z. X. (2019). Liquid crystal Enabled Dynamic Cloaking of Terahertz Fano Resonators. *Appl. Phys. Lett.* 114, 041106. doi:10.1063/1.5082224

Suen, J. Y. (2016). Terabit-per-second Satellite Links: a Path toward Ubiquitous Terahertz Communication. *J. Infrared Milli Terahz Waves* 37, 615–639. doi:10.1007/s10762-016-0257-x

Wang, T., Zhang, H., Zhang, Y., Zhang, Y., and Cao, M. (2020). Tunable Bifunctional Terahertz Metamaterial Device Based on Dirac Semimetals and Vanadium Dioxide. *Opt. Express* 28, 17434–17448. doi:10.1364/oe.394784

Zhang, F. (2017). All-dielectric Metasurfaces for Simultaneous Giant Circular Asymmetric Transmission and Wavefront Shaping Based on Asymmetric Photonic Spin–Orbit Interactions. *Adv. Funct. Mater.* 27, 1704295. doi:10.1002/adfm.201704295

Zheng, W. (2009). Observation of Unidirectional Backscattering-Immune Topological Electromagnetic States. *Nature* 461, 772.

Zhou, Z. K. (2021). Switchable Bifunctional Metamaterial for Terahertz Anomalous Reflection and Broadband Absorption. *Phys. Scr.* 96. doi:10.1088/1402-4896/ac1842

Zhu, Y., Zhao, Y., Holtz, M., Fan, Z., and Bernussi, A. A. (2012). Effect of Substrate Orientation on Terahertz Optical Transmission through VO_2 Thin Films and Application to Functional Antireflection Coatings. *J. Opt. Soc. Am. B* 29, 2373–2377. doi:10.1364/josab.29.002373

Conflict of Interest: The authors declare that the research was conducted in the absence of any commercial or financial relationships that could be construed as a potential conflict of interest.